ChemComm

In-situ Fabrication of Fully Negatively-charged Layer-by-layer Nanofilms on a Living Cell Surface

Journal:	*ChemComm*
Manuscript ID	CC-COM-06-2024-002782
Article Type:	Communication

Data availability statements

The data supporting this article have been included as part of the Supplementary Information.

ChemComm

COMMUNICATION

In-situ Fabrication of Fully Negatively-charged Layer-by-layer Nanofilms on a Living Cell Surface

Received 00th January 20xx,
Accepted 00th January 20xx

DOI: 10.1039/x0xx00000x

Zhuying Zhang[a] Jinfeng Zeng [a] and Michiya Matsusaki*[a]

Fully negatively-charged (FNC) layer-by-layer nanofilms were successfully assembled on a living cell surface for the first time using only poly acrylic acid (PAA) by introducing strain-promoted click chemistry to crosslink PAA layers. The resulting nanofilms retained their negative charges and showed higher adsorption of positively-charged molecules without affecting the cell viability.

In the early 1990s, Decher and co-workers successfully realized layer-by-layer (LbL) assembly of oppositely charged polyelectrolytes.[1] Ever since then, this method has been extensively applied to fabricate multilayered nanofilms. Among the various driving forces, electrostatic interactions remain the main method of driving the alternate deposition of polyanions and polycations.

The assembly between polyanions and polycations consumes the charges, making the nanofilms retain only the surface charges. To maintain the charges along the polyelectrolytes and ensure the nanofilm retains a high charge density, LbL between polymers with same kind of charge is necessary. However, electrostatic repulsion prevents the direct assembly of the same polyelectrolytes. Therefore, new interactions to overcome electrostatic repulsions are required. Copper-catalysed azide-alkyne cycloaddition (CuAAC) can react efficiently at room temperature and forms stable triazole. This makes it suitable for new interactions. Caruso group has demonstrated CuAAC can successfully overcome the electrostatic interaction in LbL.[2,3] Recently, our group also fabricated fully single-charged LbL nanofilms using negatively-charged poly (acrylic acid) (PAA) as the backbone and CuAAC as the driving force to overcome electrostatic repulsion.[4] Compared to polyelectrolyte (PE) LbL nanofilms, the fully negatively-charged (FNC) nanofilms showed extraordinary pH-responsive properties and high capacity of loading positively-charged molecules due to the high negative charge density.

However, the requirement of cytotoxic copper ions[5,6] limits the application of in-situ LbL assembly of FNC nanofilms on the cell surface. In-situ LbL on a cell surface has wide applications like cell compartmentalization[7] and increasing the cell viability.[8] Strain-promoted alkyne-azide cycloaddition (SPAAC) of azide and cyclooctyne as a copper-free and biorthogonal click reaction can occur in living cells without interfering with normal cellular processes.[9] Due to the high selectivity and no additional reagents, this reaction is a useful tool to realize in-situ LbL assembly on a cell surface. In this study, we chose negatively-charged PAA as the polymer backbone, and exploited the reactivity between azide and dibenzocyclooctyne

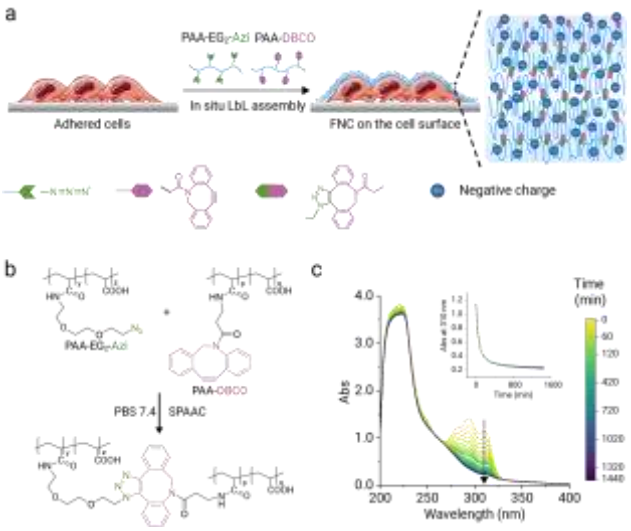

Fig. 1 (a) Schematic illustration of in situ LbL assembly of Cu-free FNC LbL nanofilms on cell surface based on SPAAC reaction. (b) SPAAC reaction between PAA-EG_2-Azi and PAA-DBCO. (c) Absorbance spectra throughout the SPAAC reaction. Inserted: absorbance time series at 310 nm. The reaction was run with 0.16 mg/mL PAA-DBCO and 1.6 mg/mL PAA-EG_2-Azi in PBS 7.4.

[a] Department of Applied Chemistry, Graduate School of Engineering, Osaka University, 2-1 Yamadaoka, Suita, Osaka 565-0871, Japan. Email: m-matsus@chem.eng.osaka-u.ac.jp

Electronic Supplementary Information (ESI) available: [details of any supplementary information available should be included here]. See DOI: 10.1039/x0xx00000x

(DBCO) under physiological conditions to deposit Cu-free FNC LbL nanofilms on living cell surfaces (Fig. 1a). We suggest that covalent binding of azide and DBCO can overcome the electrostatic repulsion between deprotonated carboxyl groups of PAA. Compared to the traditional PE films, the FNC nanofilms with high charge density have been proved to show higher loading capacity to positive-charged molecules,[4] that can be used for the drug and growth factor loading in tissue engineering. The FNC nanofilms avoid the use of polycations, which are cytotoxic by disrupting cell membrane.[10] Even the outmost layer negative-charged, the leakage polycations from the PE nanofilms in the physiological environment remains a risk. The fabrication and further application of FNC LbL nanofilms avoid the cytotoxicity of polycations. To the best of our knowledge, this is the first research to report fabrication of FNC LbL nanofilms on living cell surfaces.

We first conjugated azide and DBCO to polyacrylic acid (PAA), a negatively-charged polyelectrolyte. Briefly, the carboxyl groups of PAA were activated using (4,6-Dimethoxy-1,3,5-triazin-2-yl)-4-methyl morpholinium chloride (DMTMM) as a coupling agent, then conjugated to Azi-EG_2-amine and DBCO amine, respectively (Fig. S1). ^{1}H-NMR spectra confirmed the successful synthesis of PAA-EG_2-Azi with a 21% graft ratio and PAA-DBCO with a 9% graft ratio (Fig. S2). The SPAAC reaction between the two polymers was confirmed by UV-vis spectrophotometry. PAA-EG_2-Azi (final concentration: 1.6 mg/mL) and PAA-DBCO (final concentration: 0.16 mg/mL) were mixed in a PBS 7.4 and the reaction was monitored by observing the change in the UV-vis spectrum of the mixture. The UV-vis absorbance was measured every 10 min for the first 2 h, then every 30 min thereafter. As the reaction proceeded, the characteristic absorbance peak of DBCO at 310 nm gradually decreased (Fig. 1c) due to the structural change of a cyclooctyne into a triazole (Fig. 1b).

The fabrication of FNC LbL nanofilms was based on the efficient and irreversible SPAAC between PAA-EG_2-Azi and PAA-DBCO. By alternately exposing the substrate to different functionalized polymer solutions, the SPAAC reaction led to the absorption of polymer to the pre-layer (Fig. 2a). LbL assembly of the nanofilms was monitored by quartz crystal microbalance (QCM). As expected, the frequency shift (ΔF) increased with the alternate exposure of the QCM sensor to PAA-EG_2-Azi and PAA-DBCO (Fig. 2b and Fig. S3), confirming the layer-by-layer deposition of polymers. The 5-bilayer nanofilm showed a total ΔF of 1,074 Hz. Unlike PE LbL nanofilms that dissociate when the pH breaks the electrostatic interactions between layers,[4] the Cu-free FNC nanofilms were able to maintain the interactions even in a harsh pH environment due to the covalent bonding between the azide and DBCO (Fig. 2c), showing good stability.

The LbL nanofilms contained a large number of free carboxyl groups, which are sensitive to pH changes. When we changed the pH of the PBS on the QCM sensors, the ΔF showed a cyclic fluctuation between the average value of 964 and 494 Hz (Fig. 2d), indicating the swelling of FNC nanofilms at pH 7.4 and shrinking at pH 6.5. The thickness and surface roughness of the 5-bilayer nanofilm was evaluated by AFM at different pH (Fig. 2f and g). The height profile revealed the thickness of the nanofilm

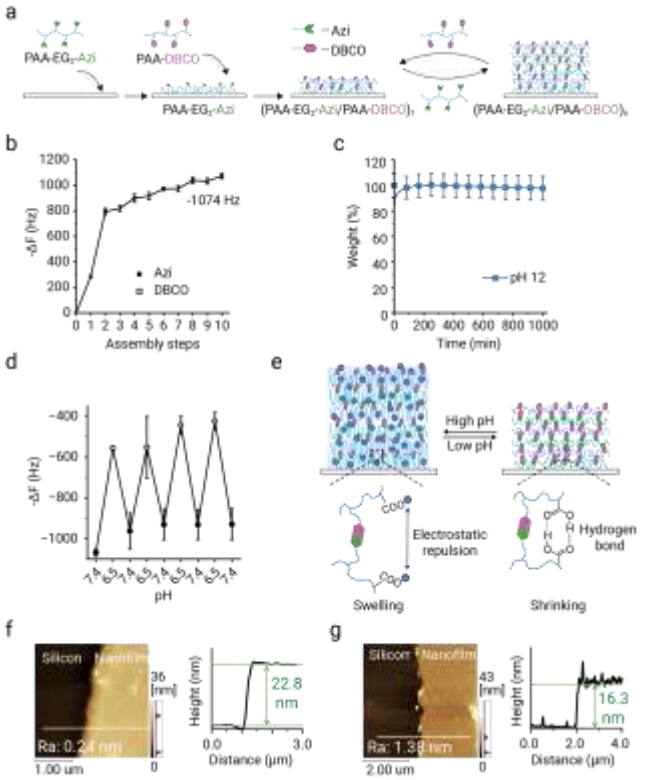

Fig. 2 Characteristics of Cu-free FNC LbL nanofilms (a) Schematic illustration of Cu-free FNC LbL nanofilm fabrication (b) Frequency shifts (ΔF) of (PAA-EG_2-Azi/PAA-DBCO)$_5$ LbL nanofilm at each step (n=3). (c) Stability of (PAA-EG_2-Azi/PAA-DBCO)$_5$ LbL nanofilm incubating in pH 12 solutions. (d) Frequency shifts (ΔF) of (PAA-EG_2-Azi/PAA-DBCO)$_5$ LbL nanofilm in PBS 7.4 and PBS 6.5. (e) Schematic depicting the pH responsive properties. (f-g) AFM height image of (PAA-EG_2-Azi/PAA-DBCO)$_5$ LbL nanofilm in PBS 7.4 (f) and PBS 6.5 (g) and the corresponding height profile across the scratched edge and surface roughness (Ra). The concentration of the polymer is 0.16 mg/mL.

was 22.8 nm in PBS 7.4 and 16.3 nm in PBS 6.5. The results showed the same trend as the QCM measurement. Additionally, nanofilms in PBS 7.4 (Ra: 0.24 nm) showed a lower surface roughness than in PBS 6.5 (1.38 nm) (Fig. 2f and g, Fig. S4). With the pKa of PAA around 4.5[11], the pH sensitivity was related to the ratio of protonated and deprotonated free carboxyl groups in the nanofilms. As shown in Fig. 2e, higher pH increased the ratio of deprotonated carboxyl groups, increasing both intermolecular and intramolecular electrostatic repulsion, leading to a swelling of the nanofilms. Conversely, lower pH resulted in less repulsion, and increase the hydrogen bond between some protonated carboxyl groups, allowing the nanofilms to shrink and form a more collapsed polymer conformation[12,13] on the surface of the agglomerates.

Next, we investigated the possibility of in situ LbL assembly directly on the cell surface. To better observe the nanofilm deposition, both PAA-EG_2-Azi and PAA-DBCO were labeled with FGA and Cy5-amine via DMTMM mediated reaction, respectively (Fig. S5a and S6a). The conjugations of fluorescent reagents were confirmed by measuring the fluorescence spectra (Fig. S5c and S6c) of polymer solutions and CLSM observation (Fig. S4d and S5d). By measuring the standard curves (Fig. S5b and S6b) of FGA and Cy5-amine monomers, the conjugating percentage of FGA to PAA-EG_2-Azi and Cy5-amine

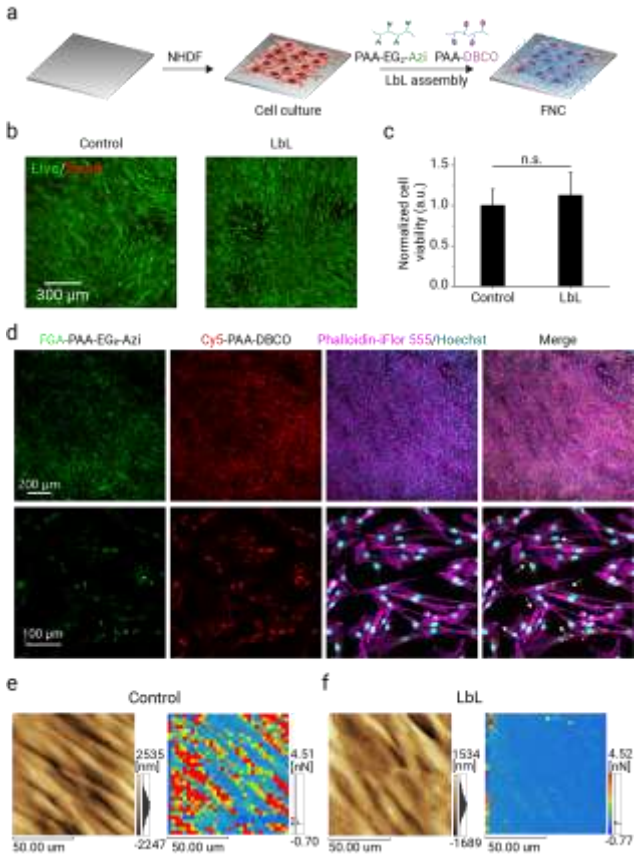

Fig. 3 Cu-free FNC LbL nanofilms in situ assembled on cell surface. (a) Schematic image of LbL assembly process of $(PAA\text{-}EG_2\text{-}Azi/PAA\text{-}DBCO)_5$ nanofilms on cell surface. (b) CLSM images of living cells stained by Calcein AM (green) and dead cells stained by ethidium homodimer-1 (red). (c) Normalized cell viability after 24 h incubating without (Control) and with (LbL) nanofilms assembled on the cell surface. Data are presented as means ± S.D. Statistical analysis was performed using Student t-test. (n.s. $p \geq 0.05$) (d) CLSM images of the $(FGA\text{-}PAA\text{-}EG_2\text{-}Azi/Cy5\text{-}PAA\text{-}DBCO)_5$ LbL nanofilms deposited on the cell surface and then incubated for 24 h. (Green: FGA, red: Cy5, violet: Phalloidin-iFlor 555, cyan: Hoechst). White arrows indicated the overlapping of nanofilms and cells. The concentration of the polymer is 0.16 mg/mL. (e-f) AFM height images (left) and adhesive force map (right) of the same cell surface area without nanofilms (e) and with nanofilms (f). Cells were fixed with 4% PFA and were measured in PBS 7.4.

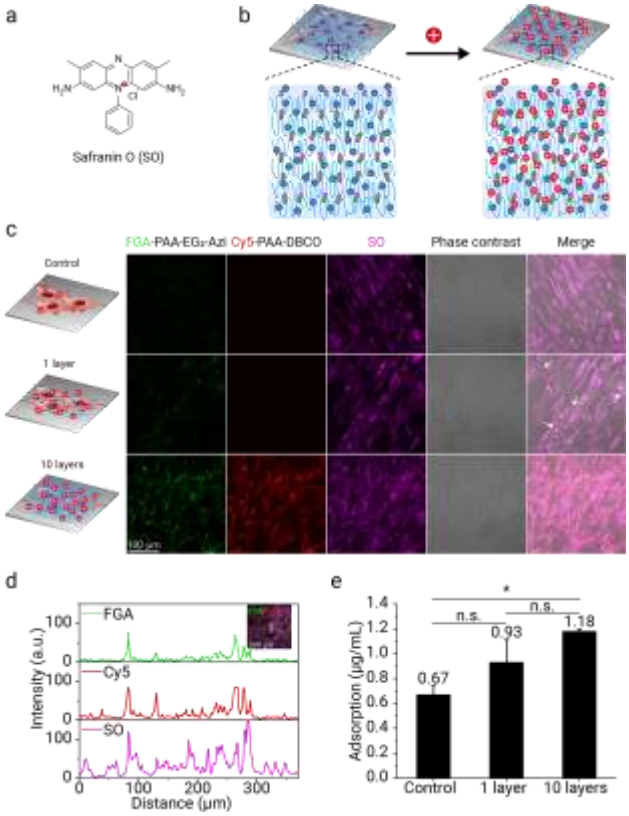

Fig. 4 Absorption properties of Cu-free FNC LbL nanofilms on cell surface. (a) Molecular structure of Sarafin O (SO). (b) Scheme illustration showing the absorption of SO by FNC nanofilms. (c) CMSL images of cells without nanofilms (control, upper line), with $PAA\text{-}EG_2\text{-}Azi$ (1 layer, middle line) and $(PAA\text{-}EG_2\text{-}Azi/PAA\text{-}DBCO)_5$ (10 layers, lower line) obtained after 30 min incubation in the solutions of SO (10 μg/mL). (Green: FGA, red: Cy5, violet: SO). (d) Linear scanning of the fluorescence intensity profiles along the white line of the inserted image after 30 min incubation in SO. (e) The uptake of SO by the 10 layers, 1 layer of nanofilms deposited on the cells and cells without nanofilms, respectively. Data are presented as means ± S.D. Statistical analysis was performed using one-way *ANOVA*. (n.s. $p \geq 0.05$; *$p < 0.05$)

to PAA-DBCO were calculated to be 0.1% and 0.01%, respectively. LbL assembly of the fluorescence labeled polymers was also monitored by QCM (Fig. S7). Fluorescence labeled polymers showed the same assembly behavior as the non-fluorescence labeled polymers, the total ΔF of $(FGA\text{-}PAA\text{-}EG_2\text{-}Azi/Cy5\text{-}PAA\text{-}DBCO)_5$ LbL nanofilms was 1,169 Hz, close to the 1,074 Hz of the nanofilms fabricated by non-fluorescent polymers. The LbL deposition of $FGA\text{-}PAA\text{-}EG_2\text{-}Azi$ and Cy5-PAA-DBCO were also confirmed by measuring the fluorescence intensity at 1, 3, and 5 bilayers (Fig. S8a). As the layer numbers increased, the intensity of both FGA and Cy5 fluorescence signals increased (Fig. S8b), indicating the stepwise deposition of $FGA\text{-}PAA\text{-}EG_2\text{-}Azi$ and Cy5-PAA-DBCO.

Normal human dermal fibroblasts (NHDF) were seeded on glass-bottomed dishes then cultured for 24 h to make the cells attach to the substrates. $(PAA\text{-}EG_2\text{-}Azi/PAA\text{-}DBCO)_5$ nanofilms were assembled on the attached cells following the same protocol as on the QCM sensors (Fig. 3a). After 24 h of nanofilm deposition on the cell surface, initial viability tests were then performed via live/dead staining and WST-8 assay. Cells coated with nanofilms showed no decrease in viability compared with the control group, suggesting cytocompatibility of the nanofilms (Fig. 3b and c). We then investigated the localization of the nanofilms on the living cell surface. As shown in Fig. 3d, the polymers formed a continuous network consisting of fibers. Fluorescence signals of $FGA\text{-}PAA\text{-}EG_2\text{-}Azi$ completely overlapped with Cy5-PAA-DBCO. This observation suggested that two different functionalized PAA were localized at the same place, indicating the highly specific interaction between azide and DBCO. Nanofilm signals partially overlapped with cells after 24 h of incubation, meaning that the nanofilms interacted with the cell surface. The co-incubation for 24 h also suggests the stability of LbL nanofilms in cell culture medium. From the high magnification images, we then compared the cellular morphology, as shown in Fig. 3d and Fig. S9. CLSM images are of the LbL group and control group, where the NHDF cells showed normal cell morphology, suggesting the presence of nanofilms on the cell surface didn't affect the cell behavior.

Upon successfully confirming the in situ assembly of nanofilms on the cell surface, we next investigated whether this nanofilm coating could affect the properties of the cell surface.

Therefore, AFM was used to quantify membrane adhesion of NHDF in PBS. As shown in Fig. 3e and f, from the height images, fibers-shaped nanofilms over the cell surface and in between the gap of neighboring cells were observed after LbL assembly, matching the results shown in the CLSM images (Fig. 3d), further indicating the successful assembly of nanofilms. The maps of adhesion force exhibited heterogeneous distribution of adhesion behavior where the region around the cell's center possessed a higher adhesion force. In addition, compared with the control group, the adhesive force of the LbL group was markedly lower. The tips of the AFM probes are slightly negatively charged,[14] so after the fabrication of our FNC nanofilms on the cell surface, the cell coated with nanofilms attracted the tip less than cells without nanofilms, resulting in a decrease of adhesive force. This confirms the nanofilm can change the surface charges of cells to a more negative state. The ability to absorb positively-charged molecules might be applied to load biofactors or drugs that are used to further regulate the cell behavior. Besides, the FNC nanofilms on the surface might serve as a shell to prevent the cell being harmed by positively-charged polymers.

The abundant negative charges on the cell surface led to the expectation that nanofilms could effectively absorb positively-charged molecules. Here, we used positive-charged Safranin O (SO) as the model drug or growth factor, with a distinct emission wavelength from that of fluorescent labelled polymers to evaluate the adsorption properties of the FNC nanofilms on the cell surface. For a better comparison, we also prepared samples with only 1 layer of PAA-EG_2-Azi deposited on the cell surface. The as prepared samples were incubated in SO solutions for 30 min then the excess SO was washed away using PBS. For the control groups without nanofilms, SO can only be absorbed by the negative charges on the cell surface,[15] thus fluorescence signals only show on top in the area where the cell attached (Fig. 4c, upper line and Fig S11a). For the cells coated with only one PAA-EG_2-Azi layer (Fig. 4c, middle line), the partial overlap of polymer and SO signals can be observed (Fig S11b), indicate the adsorption of SO of the polymer layer. The cells coated with 10 layers (PAA-EG_2-Azi/PAA-DBCO)$_5$ effectively absorbed SO via electrostatic interaction on the surface (Fig. 4c, lower line) and the location where nanofilms deposited exhibited an especially high fluorescence intensity of SO which is demonstrated by the overlapped peak of the fluorescence profile of polymers and SO (Fig. 4d and Fig. S11c). Quantitative assessment of the adsorption performance of the samples during incubation of SO solutions demonstrated that the FNC nanofilms deposited on the cell surface increased the SO uptake to about 1.76 times that of the control groups.

In conclusion, we fabricated a Cu-free FNC LbL nanofilm based on SPAAC click reaction and achieved in-situ assembly on a living cell surface. We confirmed the reaction between PAA-EG_2-Azi and PAA-DBCO in PBS 7.4. LbL assembly was successfully realized both on the inorganic substrate and on a living cell surface. The FNC nanofilms showed pH responsiveness on the thickness and surface morphology. Fluorescence-labeled polymer and cell staining confirmed the successful deposition of nanofilms on the cell surfaces. AFM force mapping showed that the nanofilms markedly reduced the cell surface adhesion without affecting the cell viability and morphology. The surface modification on the cell with FNC nanofilms with abundant negative charges allows them to possess a higher capacity of positively-charged molecules for further applications. This is the first report of FNC LbL nanofilms on a cell surface.

This work was supported by SPRING (JPMJSP2138), and COI-NEXT (JPMJPF2009) from JST, JPNP20004 from NEDO, Grant-in-Aid for Scientific Research (A) (20H00665), and Grant-in-Aid for Challenging Exploratory Research (22K19918) from JSPS.

Conflicts of interest

There are no conflicts to declare.

Data availability

The data supporting this article have been included as part of the Supplementary Information.

Notes and references

1 G. Decher and J.-D. Hong, *Makromol. Chem. Macromol. Symp.*, 1991, **46**, 321–327.

2 G. K. Such, J. F. Quinn, A. Quinn, E. Tjipto and F. Caruso, *J. Am. Chem. Soc.*, 2006, **128**, 9318–9319.

3 G. K. Such, E. Tjipto, A. Postma, A. P. R. Johnston and F. Caruso, *Nano Lett.*, 2007, **7**, 1706–1710.

4 Z. Zhang, J. Zeng, W. Li and M. Matsusaki, *Chem. Mater.*, 2024, **36**, 1947–1956.

5 M. C. Cortizo and M. F. L. De Mele, *Biol. Trace Elem. Res.*, 2004, **102**, 129–142.

6 E. Mavil-Guerrero, R. Vazquez-Duhalt and K. Juarez-Moreno, *Chemosphere*, 2024, **347**, 140713.

7 J. Zeng, N. Sasaki, C. R. Correia, J. F. Mano and M. Matsusaki, *Small*, 2020, **16**, 1907434.

8 D. Choi, H. Lee, H.-B. Kim, M. Yang, J. Heo, Y. Won, S. S. Jang, J. K. Park, Y. Son, T. I. Oh, E. Lee and J. Hong, *Chem. Mater.*, 2017, **29**, 2055–2065.

9 J. C. Jewett, E. M. Sletten and C. R. Bertozzi, *J. Am. Chem. Soc.*, 2010, **132**, 3688–3690.

10 M. Wytrwal-Sarna, P. Knobloch, S. Lasota, M. Michalik, M. Nowakowska and M. Kepczynski, *Environ. Sci. Nano*, 2022, **9**, 702–713.

11 D. Yoo, S. S. Shiratori and M. F. Rubner, *Macromolecules*, 1998, **31**, 4309–4318.

12 M. Todica, R. Stefan, C. V. Pop and L. Olar, *Acta Phys. Pol. A*, 2015, **128**, 128–135.

13 D. G. Mintis and V. G. Mavrantzas, *J. Phys. Chem. B*, 2019, **123**, 4204–4219.

14 L. Li, N. F. Steinmetz, S. J. Eppell and F. R. Zypman, *Langmuir*, 2020, **36**, 13621–13632.

15 M. Nishino, I. Matsuzaki, F. Y. Musangile, Y. Takahashi, Y. Iwahashi, K. Warigaya, Y. Kinoshita, F. Kojima and S. Murata, *PLoS ONE*, 2020, **15**, e0236373.